Non-Contact Stiffness Measurement of a Suspended Single Walled Carbon Nanotube Device

Yun Zheng,[a] Chanmin Su,[b] Stephanie Getty[c]
[a] Detectors Systems Branch, NASA Goddard Space Flight Center, Greenbelt, MD 20771
[b] Veeco Instruments, Inc., 112 Robin Hill Road, Santa Barbara, CA 93117
[c] Materials Engineering Branch, NASA Goddard Space Flight Center, Greenbelt, MD 20771

ABSTRACT

A new nanoscale electric field sensor was developed for studying triboelectric charging in terrestrial and Martian dust devils. This sensor is capable to measure the large electric fields for large dust devils without saturation. However, to quantify the electric charges and the field strength it is critical to calibrate the mechanical stiffness of the sensor devices. We performed a technical feasibility study of the Nano E-field Sensor stiffness by a non-contact stiffness measurement method. The measurement is based on laser Doppler vibrometer measurement of the thermal noise due to energy flunctuations in the devices. The experiment method provides a novel approach to acquire data that is essential in analyzing the quantitative performance of the E-field Nano Sensor. To carry out the non-contact stiffness measurement, we fabricated a new Single-Walled Carbon Nanotube (SWCNT) E-field sensor with different SWCNTs suspension conditions. The power spectra of the thermal induced displacement in the nano E-field sensor were measured at the accuracy of picometer. The power spectra were then used to derive the mechanical stiffness of the sensors. Effect of suspension conditions on stiffness and sensor sensitivty was discussed. After combined deformation and resistivity measurement, we can compare with our laboratory testing and field testing results. This new non-contact measurement technology can also help to explore to other nano and MEMS devices in the future.

Keywords: Non-contact stiffness measurement, Resonant frequency, Nanotechnology, MEMS, Single-walled carbon nanotubes, Electric field sensor

1. INTRODUCTION

Mars is known to have a dynamic atmosphere with dust devils and global dust storms. Figure 1 shows a dust devil observed by NASA's Sprit Rover on Mars in 2007. Dust devils can produce locally large electric field which is important for Martian's atmosphere and weather. To understand the magnitude of electric fields associated with these dust devils can provide substantial insight into the interplay of atmospheric chemistry and weather near the Martian surface. Terrestrial dust devils are known as dry cyclones originating from temperature inversion, such as a hot surface and cooler air column that lift dust grains into circulation. They have been recognized to support substantial electric fields (E-Fields) due to grain-gain contact electrification [1]-[2]. Comparison to their terrestrial cousins indicates the presence of large tribocharged electric fields within their structure. The electric fields in terrestrial dust devils can be of order 10^4 to 10^5V/m, large enough to saturate commonly used electric field mills. Farrell etc. reported a new design for an electric field sensor that can operate at high field [2,3].

Furthermore, a miniaturized design has been employed to offer mass and power savings for a future in situ planetary science mission [4].

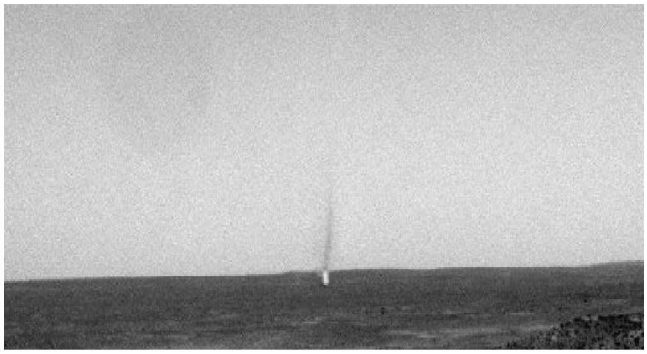

Figure 1. Dust devils observed by Spirit Rover on Mars in 2007.

To miniaturize a device or a sensor, nanotechnology and microelectromechanical systems (MEMS) technology present promising routes to novel miniaturized devices. Single-walled carbon nanotubes, in particular, exhibit an unusually high degree of piezoresistance, or change in electronic properties with mechanical strain. We have previously reported [4] the development of a prototype electric field sensor using microfabrication methods and employing the piezoresistance of single-walled carbon nanotubes. As designed, the operational schematic is shown in Figure 2. The electrical field sensor consists of a gold needle as conductor suspended by a network of SWCNTs. The network of SWCNTs is connected between two gold electrodes across a trench in a silicon substrate. When the sensor is placed in an electric field it will generate an electric dipole on the surface of the conductor, which is mechanically coupled to the SWCNTs. Applied bias voltage on the silicon substrate below the sensor will electrostatically deflect the conductor, which results in deflection of the SWCNT network. Since the SWCNTs are piezoresistive, their electrical conductance is expected to be reduced by the application of strain. Therefore, deflection of the suspended structure can be transduced into an electronic signal.

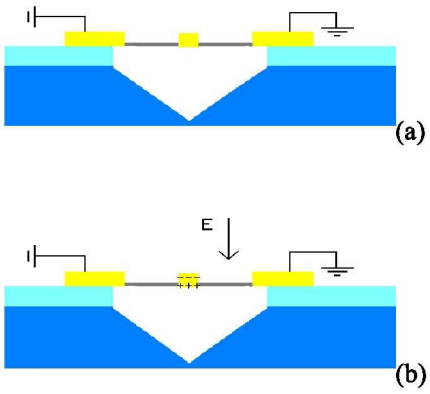

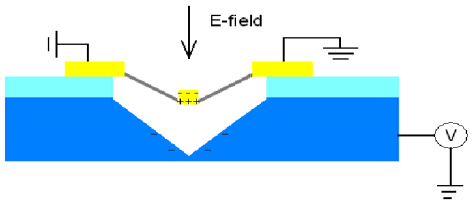

Figure 2. Schematic diagram of nano e-field sensor measuring electric field. (a) Apply voltage between two electrodes to measure conductance. (b) An applied field couples to the device through polarization of the gold deflector. (c) The biased substrate pulls on the needle, which generates strain to the SWCNTs and causes a change in device conductance.

The prototype was tested in the laboratory and in a field campaign to measure the electric field of dust devils. During field testing, we observed that the Nano E-field Sensor device resistance was found to be correlated with peaks in a control electrometer signal [Fig. 3], indicating a response to external electric field.

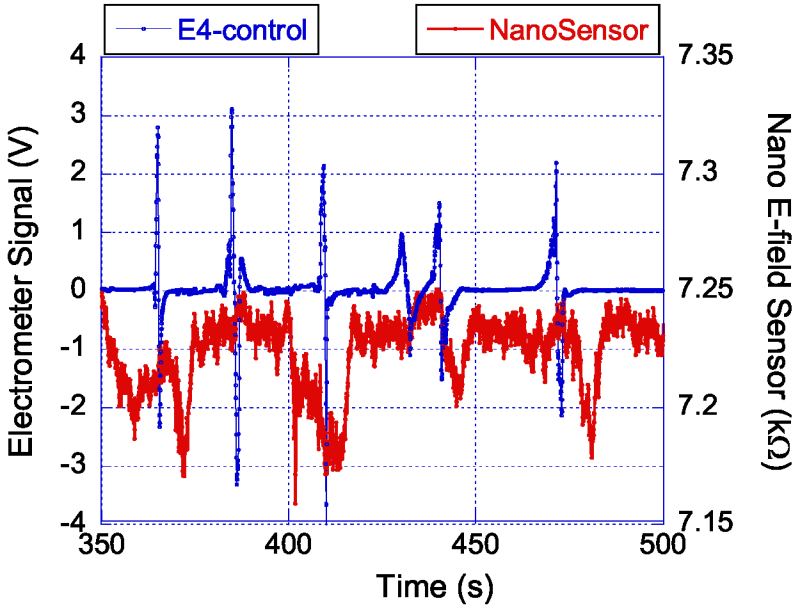

Figure 3. Field testing data of the Nano E-field Sensor (red) and control electrometer (blue). Deviations in nano E-field sensor at time 370 s, 410 s, 445 s, and 480 s show some correlation with peaks in the control signal.

However, to quantitatively characterize the electric field response, we need to know the deformation and stiffness of the SWCNTs. Hutter et al. [5] proposed a new method to determine the mechanical properties of a suspended device by using thermal noise induced cantilever motion to determine its spring constant. In this method the power spectral density of the thermal induced displacement was analyzed using equipartition theorem, yielding a spring constant inversely proportional to the maximum at the resonance [6]. This method involves no drive actuation coupling, no contact interaction and requires no knowledge of the cantilever geometry. However, due to laser spot size, strong dependency of the deflection sensitivity on laser positioning, uncertainty of the accuracy of the displacement calibration, and the noise of the measurement system, the accuracy of the technique needs refinement. Recently, a new non-contact stiffness measurement method was developed using a heterodyne laser interferometer

with a displacement resolution of $2.6 \times 10^{-15} m/(Hz)^{1/2}$. This method provides precise measurements of the scanning probe cantilevers with spring constants ranging from mN/m to tens of N/m [7]. Nano E-field sensor non-contact stiffness measurement will explore this new technology in broader application to NEMS and MEMS devices.

2. EXPERIMENTS

2.1 E-Field Sensor

E-field sensor fabrication was carried out using carbon nanotube growth facilities and device fabrication tools housed in a class 10 clean room with MEMS fabrication facilities at NASA's Goddard Space Flight Center. To fabricate the nano E-field sensor, single-walled carbon nanotubes were grown on an oxidized silicon substrate by a chemical vapor deposition (CVD) at 950°C. Figure 4 shows single-walled carbon nanotube growth on the silicon oxide.

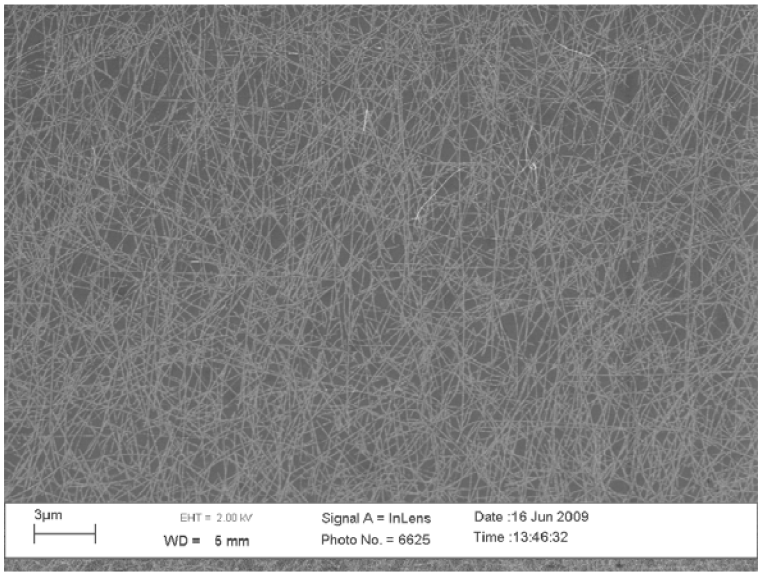

Figure 4. SEM picture of single walled carbon nanotube on silicon substrate before fabricate electrical sensor.

The length of the SWCNTs can be considerably more than 10 micron, and they are randomly distributed to form a dense single-walled carbon nanotube network. After growth, photolithographic patterning was used to form a gold needle and electrodes. Finally, wet etching was used to form a trench underneath of the gold needle. Four E-field sensor devices, sample P1, P2, P3 and P4, were fabricated in a 10mm x 10mm silicon substrate. Among of them, sample P2 was damaged during the fabrication. Sample P1, P3 and P4 were fabricated with different suspension conditions in order to better understand the effect on stiffness and E-field sensor sensitivity.

Figure 5 shows a fabricated E-field sensor sample P4. It can be seen from the figure that the gold needle deflector is successfully suspended between two gold electrodes on a SWCNTs

network above a silicon trench. The electrodes serve to clamp the ends of the SWCNTs to the underlying substrate. In the E-field sensor sample P3 both ends of deflector are connected with a thin layer of silicon oxide to the substrate [Fig. 6]. In E-field sensor sample P1, one end of deflector is partially connected with a thin layer of silicon oxide to the substrate and also with a thin layer of silicon oxide to the gold electrode. P1 is therefore effectively clamped at approximately the center and at one end.

In the three different suspension conditions, density of SWCNTs networks of the E-field sensors is expected to be negligible. The measurement results of the three different suspension conditions of E-field sensor can give us a better understanding of how the suspension condition affects the sensitivity of the E-field sensor. Assuming nominally comparable SWCNT density for all three devices, P4 is expected to exhibit the lowest stiffness, moderate stiffness is expected for P3, and the highest stiffness is expected for P1.

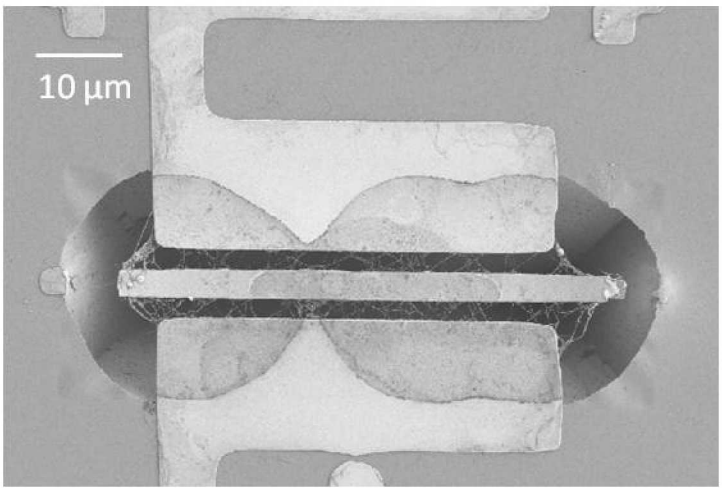

Figure 5. SEM picture of a completed nano E-field sensor sample 4. The opposing electrodes mechanically retain the SWCNTs. The central device, delineated by the rounded trench outline, is suspended from the substrate. The deflector is supported entirely by the SWCNT network.

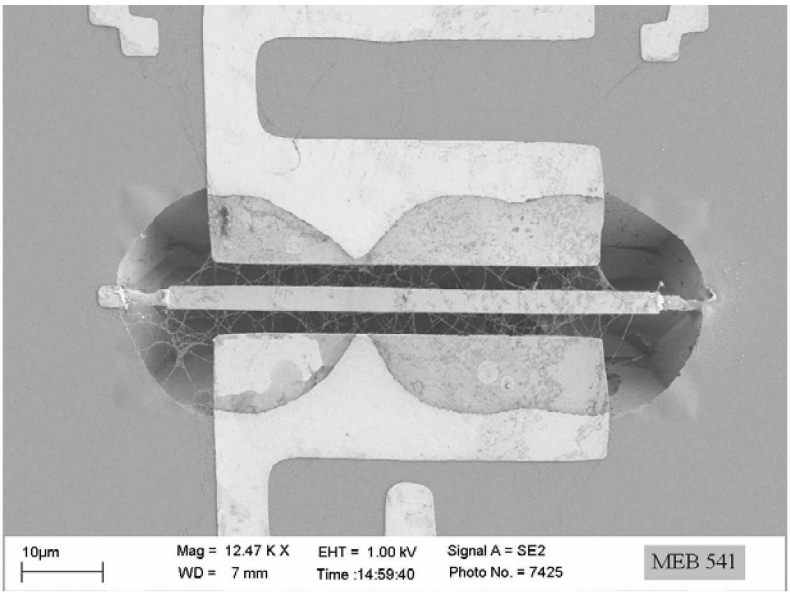

Figure 6. SEM picture of E-field sensor sample P3. Both ends of gold deflector are connected with a thin layer of SiO_2 to the substrate.

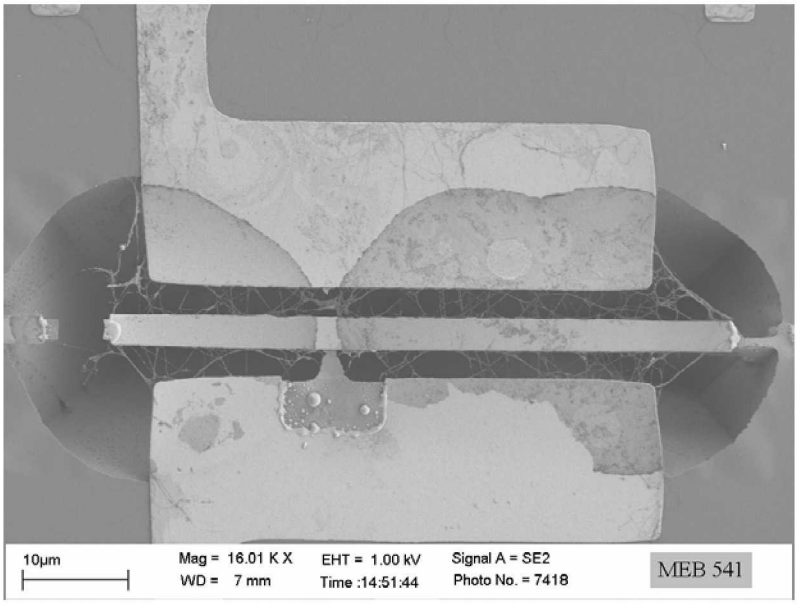

Figure 7. SEM picture of E-field sensor sample P1. One end of deflector is partially connected with a thin layer of SiO_2 to the substrate. The middle of deflector is partially connected to gold electrode.

2.2 Non-contact stiffness measurement

The non-contact stiffness measurements were carried out using a Laser Doppler Vibrometer (Polytec GmbH). The displacement gauge of the Doppler Vibrometer is traceable to

EUROMET. In order to study the effect of suspension conditions on the nano E-field sensor stiffness, we measured E-field sensors in different suspension conditions, sample P1, P3 and P4.

To carry out the non-contact stiffness measurement, the E-field sensor substrate was placed on the stage of laser Doppler vibrometer. The laser beam was carefully adjusted to the smallest point, about two micron. The laser beam was focused on the middle of the gold needle deflector. Figure 8 shows measurement set up and the non-contact stiffness measurement of nano E-field sensor. The image on computer screen showed measurement of E-field sensor sample P4. After measurement the data were processed and analyzed with using the algorithm developed by Rast et al [6]. Thermal fluctuation induced displacement spectra can be plot as a function of frequency. The resonant frequecies and stiffnesses in different vibration modes are also calculated by fitting the noise power spectra data.

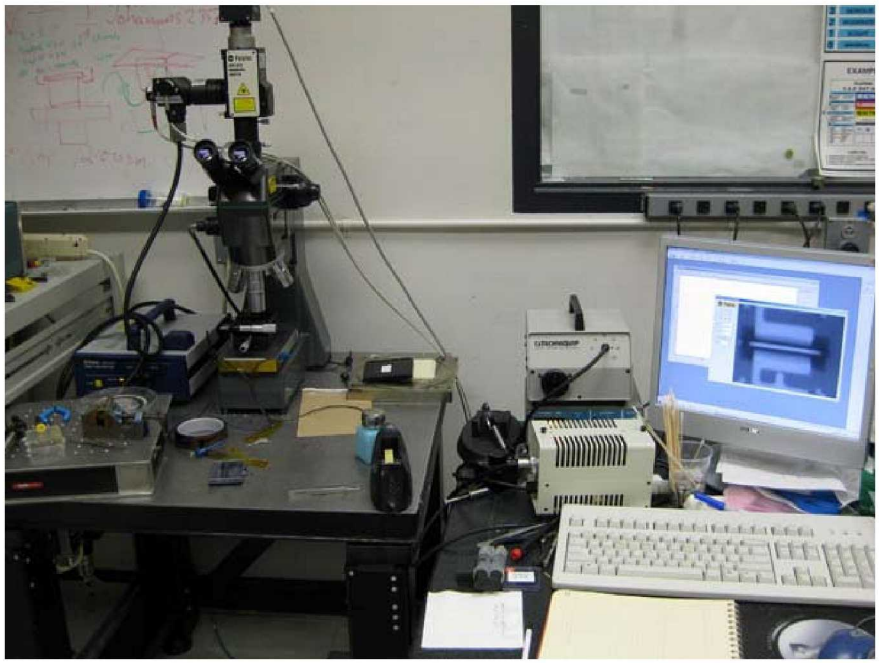

Figure 8. Non-contact stiffness measurement of E-field sensor.

3. RESULTS

The spring constant of the lever or any micromechanical components can be measured by the thermal tune method. In this method the displacement power spectra distribution $<u^2>$ in the micro-lever was measured by a laser vibrometer. Using equal partition theory the dynamic energy in the fundamental vibration mode should be determined by the following equation: [6]

$$< u^2 >= \frac{2k_B T}{\pi} \cdot \frac{Q\Delta\omega}{\omega_o k} \quad \text{.....(1)}$$

where $<u^2>$ represents the displacement power spectra, k_B the Boltzmann constant, T the absolute temperature, Q the mechanical quality factor, ω_o the resonance frequency and $\Delta\omega$ the bin size of the power spectra. The displacement measurement is calibrated according to the laser wavelength which can be easily traceable to National Institute of Standards and Technology specifications or its counterpart in Europe. On the drive force part the thermal drive energy depends only on the absolute temperature and fluctuation in the sub-degree temperature error will only cause the measurement error in the low third digit. Figure 9 shows a snap-shot of the thermal noise power spectra measurement of mode 2 in E-field sensor sample P1. The dotted line is the original measurement data of the thermal noise spectra. The solid line represents the fitted data according to equation 1. The vertical axis is power spectral density and the unit is m^2/Hz. From figure 9 we can see that this new method can measure the thermal noise in 1E-27 level. Precision of the measurement is very important for nanoscale deflections. From the thermal fluctuation induced displacement spectra we can obtain resonant frequencies in different modes.

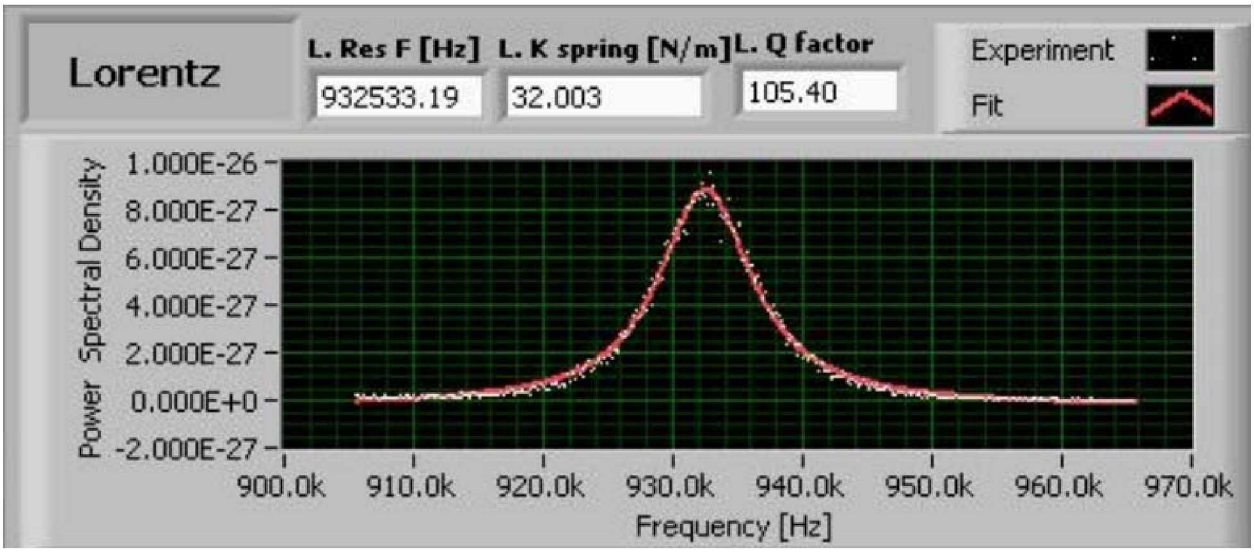

Figure 9. A snap-shot of the thermal noise power spectra measurement of mode 2 in sample P1, showing as an example. The dotted line is the original measurement data of the thermal noise spectra. The solid line represents the fitted data according to equation 1. The unit on the vertical axis is in m^2/Hz.

Table 1 shows resonant frequencies and stiffness in different vibration modes of E-field sensors sample P1, P3 and P4. Mode 1 in the table is fundamental resonant frequency, which has largest magnitude and lowest vibration frequency in the thermal fluctuation induced displacement spectra. Mode 2 is the second harmonic frequency and Mode 3 is the third harmonic frequency. In the sample P4 the gold needle deflector is fully suspended by the SWCNTs network as showed in figure 5. The measurement result in sample P4 indicated the stiffness of only SWNT network. In the sample P3 the gold needle is suspended not only by the SWCNT network but also thin silicon oxide layers at both ends of the needle deflector. Device P3's stiffness and resonant frequency results are the combination of SWCNT network and partially connected silicon oxide layer. The stiffness value of sample P3 is much larger than that of sample P4, reflecting the SWCNT network alone. In the sample P1, the gold needle deflector is suspended by SWNTs net and it also connected with silicon oxide layers at one end deflector and at the center of the deflector. It is expected the vibration is different since the focus point of

Laser Doppler Vibrometer is on the center of deflector. The stiffness of the sample P1 is almost five times higher than that of sample P4.

Table 1. Resonant frequencies in different modes and stiffness of SWCNTs net in samples P1, P3 and P4

E-field Sensors	Mode 1 (kHz)	Stiffness, M1 (N/m)	Mode 2 (kHz)	Stiffness, M2 (N/m)	Mode 3 (kHz)	Stiffness, M3 (N/m)
P1	880	49.06	933	32.2	1110	129.4
P3	1211	25.7	1321	183		
P4	678	10.7	989	21.6	1320	183.7

From the table we can see that, in a good suspended deflector, stiffness of the SWCNTs network in the E-field sensor is 10.7 N/m. If the deflector connects to substrate with silicon oxide, the stiffness can be much larger, 25.7 N/m, like the measurement results of sample P3 in the table 1. For electro-mechanical sensor, a lower spring constant or stiffness will give better sensitivity. As an E-field sensor, the lower stiffness of SWCNT network is, the better it transducer electrical field force to mechanical strain, which result in a larger conductance change. For the sample P3, which connects both ends to substrate, the stiffness is nearly 2.5 times larger than sample P4. If deflector of E-field sensor is partially connect in the center area, the stiffness is about 5 times larger than that of a fully SWCNT network suspended E-field sensor.

4. CONCLUSIONS

We have demonstrated that this new non-contact stiffness measurement technology can be used in nano and MEMS devices, especially for devices which can not measure by traditional contacted technology. In the non-contact measurement of nano E-field sensor, we obtained measurement resolution of power spectral density less than 1E-27. From the measurements we obtained stiffness and resonant frequencies of E-field sensors in different suspension conditions. After combined future deformation measurement and resistivity measurement, we can compare with our laboratory testing and field testing results. This new non-contact measurement technology can explore to other nano and MEMS devices in the future.

5. ACKNOWLEDGEMENT

This work was supported by the NASA Goddard Space Flight Center Innovative Partnerships.

6. REFERENCES

[1] Freier, G.D., "The electric field of a large dust devil," J. Geophys. Res., vol.5, no 10, p.3504, Oct. 1960.

[2] Farrell, W.M., et al., "Electric and magnetic signatures of dust devils from the 2000-2001 MATADOR desert tests," J. Geophys. Res., vol. 109, no E3, p.E03004, 2004.

[3] Jackson, T.L., Farrell, W., "Electrostatic fields in dust devils: an analog to mars," IEEE transaction on Geoscience and remote sensing, vol. 44, no.10, p.2942, Oct. 2006.
[4] Zheng, Y., King, T., Stewart, D., Getty, S., "Fabrication of a Nanoscale Electric Field Sensor," SPIE, "Proceedings of the SPIE **7318"**, 731815 (2009).
[5] Hutter, J., Bechhoefer, J., "Review of Scientific Instruments", 64 (7), 1868-1873, (1993).
[6] Rast, S., Wattinger, C., Gysin, U.,Meyer, E., "Nanotechnology" 11, 169–172 (2000).
[7] Su, C., Fischl, R., Shi, J., Belikov, S., "Quantitative Measurement of Cantilever Spring Constant Using Heterodyne Interferometer", J. Nanosci. Nanotechnol. 9, 736-40 2009.